Structure of Phenoxazinone Synthase from *Streptomyces antibioticus* Reveals a New Type 2 Copper Center[†,‡]

Alex W. Smith,[§] Ana Camara-Artigas,[||] Meitian Wang,[§] James P. Allen,*[,§] and Wilson A. Francisco*[,§]

Department of Chemistry and Biochemistry, Arizona State University, Tempe Arizona 85287-1604, and Department of Physical Chemistry, Biochemistry and Inorganic Chemistry, University of Almería, Carretera Sacramento, Almería, Spain

Received December 14, 2005; Revised Manuscript Received February 15, 2006

ABSTRACT: The multicopper oxidase phenoxazinone synthase (PHS) catalyzes the penultimate step in the biosynthesis of the antibiotic actinomycin D by *Streptomyces antibioticus*. PHS exists in two oligomeric forms: a dimeric form and a hexameric form, with older actinomycin-producing cultures containing predominately the hexameric form. The structure of hexameric PHS has been determined using X-ray diffraction to a resolution limit of 2.30 Å and is found to contain several unexpected and distinctive features. The structure forms a hexameric ring that is centered on a pseudo 6-fold axis and has an outer diameter of 185 Å with a large central cavity that has a diameter of 50 Å. This hexameric structure is stabilized by a long loop connecting two domains; bound to this long loop is a fifth copper atom that is present as a type 2 copper. This copper atom is not present in any other multicopper oxidase, and its presence appears to stabilize the hexameric structure.

Actinomycin D, one of the most potent antineoplastic agents known, is synthesized by the actinomycete *Streptomyces antibioticus*. This compound inhibits DNA-dependent RNA synthesis by intercalation of the phenoxazinone chromophore to DNA. The last step in the biosynthesis of actinomycin D, namely, the oxidative condensation of two molecules of 3-hydroxy-4-methylanthranilic acid pentapeptide lactone to form actinocin (Scheme 1), is catalyzed by the enzyme phenoxazinone synthase (PHS).[1] PHS is a multicopper oxidase produced in two distinct oligomeric forms: low activity dimers and high activity hexamers (*1*). The relative amount of the two forms is regulated; young cultures that do not produce actinomycin predominantly contain the dimeric form, whereas older actinomycin-producing cultures mostly contain the hexameric form (*1*). The dimers and hexamers are distinct stable molecular forms and are not related by a simple equilibrium-aggregation phenomenon (*1*). The regulation and structural differences between these two oligomeric forms is currently unknown.

Multicopper oxidases are an important class of enzymes found in all kingdoms of life that couple the one-electron oxidation of organic and inorganic substrates to the four-electron reduction of dioxygen to water (*2*). The most studied and characterized members of this family are laccase, ascorbate oxidase, and ceruloplasmin, all isolated from eukaryotic organisms. Recently, a small number of bacterial members of this family have been characterized, including CueO from *E. coli* (*3*) and a spore-coat laccase (CotA) from *Bacillus subtilis* (*4*). Multicopper oxidases contain three conserved copper-binding motifs: type 1 (blue), type 2 (normal), and type 3 (binuclear) centers. The type 2 and 3 copper centers form the trinuclear cluster seen in all multicopper oxidases with known structures, and this cluster is the site of oxygen binding and reduction (*5*, *6*). Although multicopper oxidases catalyze two distinct reactions, the oxidation of organic and inorganic substrates and the reduction of dioxygen to water, the latter reaction has received the most attention and has been extensively studied because of its importance in biological systems and its possible implications for energy conversion. Even with all of the experimental and theoretical information currently available, the mechanism of dioxygen reduction by multicopper oxidases is far from being completely understood.

Scheme 1: Reaction Catalyzed by PHS

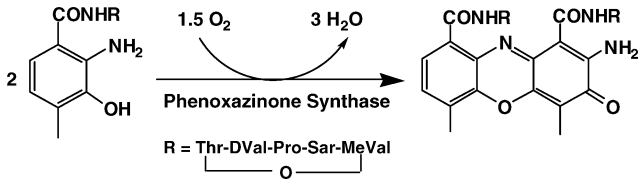

The oxidative coupling of the two molecules of substituted 2-aminophenol to produce the phenoxazinone chromophore involves a six-electron oxidation that is thought to take place in a series of three two-electron oxidations, unique among the multicopper oxidases, which usually catalyze one-electron oxidation reactions. The first two oxidation steps are proposed to occur at the active site, whereas the last two-electron oxidation takes place outside of the active site (*7*).

[†] This work has been supported in part by a grant from the National Science Foundation (MCB-0542337 to W.A.F.).

[‡] The coordinates and structure factors for the structures reported here are available from the Protein Data Bank, accession code 2G23.

* To whom correspondence should be addressed. Tel: 480-965-8241. Fax: 480-965-2747. E-mail: jallen@asu.edu (J.P.A.). Tel: 480-965-7480. Fax: 480-965-2747. E-mail: wfrancisco@asu.edu (W.A.F).

[§] Arizona State University.

[||] University of Almería.

[1] Abbreviations: PHS, phenoxazinone synthase; CotA, spore coat laccase from *Bacillus* subtilis; GGA, galactose-glutamic acid; EPR, electron paramagnetic resonance; ICP-MS, inductively coupled plasma-mass spectrometry (ICP-MS); ALS, Advanced Light Source.

10.1021/bi0525526 CCC: $33.50
Published on Web 03/18/2006

It has been shown that PHS requires a copper stoichiometry of 4−5 Cu atoms per subunit for optimal activity. Spectroscopic studies have suggested that the arrangement of the Cu centers in PHS is different from other multicopper oxidases providing evidence for the presence of one type 1 center, with the remaining copper atoms bound as type 2 centers. These studies show no evidence for the presence of a type 3 copper center (*8*).

To gain further insight into the mechanism of the action of PHS, the nature of the copper centers, and the structural parameters that stabilize the more active oligomeric form, we have determined the 3D structure of the hexameric form of the enzyme. The structure of PHS is compared to those of other multicopper oxidases, including the bacterial enzymes CotA, pdb number 1GSK, (*9*) and CueO, pdb number 1N68, (*3*). The structure confirms the presence of a type 1 center as well as the presence of the type 2/type 3 trinuclear cluster. Furthermore, the structure of the PHS hexamer contains the predicted fifth copper atom, which is part of a new type 2 center. This fifth copper atom is bound at a loop that establishes interactions between the subunits that stabilize the hexamer. The location of the fifth copper center and the requirement of 5 copper atoms for maximum activity suggest that the fifth copper atom is not merely advantageously bound but has a structural role as well. We propose that this Cu center might be involved in the stabilization of the highly active hexameric form of the enzyme.

MATERIALS AND METHODS

Expression and Purification. Expression and purification of PHS was conducted as previously described (*10*). Briefly, cultures of *Streptomyces lividans* harboring the plasmid pIJ702, which contains a 2.45 kb insert coding for PHS, were maintained according to Jones and Hopwood (*11*). *S. lividans* spores were grown in six 250 mL baffled flasks containing 50 mL of NZ-amine media with 50 μg/mL of thiostrepton and incubated for 48 h at 30 °C (*12*). Mycelia from the NZ-amine cultures were harvested and washed twice with 0.9% (w/v) NaCl and used to inoculate six 500 mL flasks containing 200 mL of galactose−glutamic acid (GGA) media (*13*) with 50 μg/mL of thiostrepton. The GGA cultures were incubated for 72 h, harvested, and washed three times with 0.9% (w/v) NaCl. The mycelia were resuspended in 50 mM Tris (pH 7.6), 1 mM phenylmethylsulfonyl fluoride, and lysozyme (0.2 mg/mL), incubated for 10 min, and sonicated (15 s bursts) for approximately 2 min. The sonicated solution was centrifuged, and the nucleic acids were precipitated with streptomycin sulfate. Ammonium sulfate was added slowly to the clarified solution until 25% saturation was reached, and the solution was centrifuged. The resulting pellet was dissolved in 10 mM sodium phosphate (pH 6.0) and dialyzed extensively in the same buffer. The PHS solution was further purified using a two-step column chromatography procedure with hydroxyapatite and Ultrogel AcA34 columns as the first and seconds steps, respectively. Fractions from the hydroxyapatite were analyzed for activity (*7*) and pooled. Fractions showing activity were dialyzed for 24 h against 100 mM sodium phosphate (pH 6.0) and 500 μM copper (II) chloride and followed by extensive dialysis against 100 mM sodium phosphate (pH 6.0) and 300 mM NaCl, before being loaded onto the Ultrogel AcA34 column. Fractions were analyzed using native polyacrylamide gel electrophoresis. Fractions showing activity and containing the hexameric form of PHS were combined and dialyzed against 10 mM sodium phosphate (pH 6.0). The dialyzed PHS solution was concentrated to approximately 75 mg/mL.

Electron Paramagnetic Resonance (EPR) and Inductively Coupled Plasma-Mass Spectrometry (ICP-MS) Analysis. EPR spectra were measured on a Bruker Elexsys 580 spectrometer with the frequency set at 9.40 GHz. The spectra were obtained at 125 K as an average of four scans using the following conditions for spectral acquisition: 1.02 mW of power, center field at 3000 G, and a sweep width of 1000 G. Spin counting was performed using Cu-EDTA as the standard.

Metal content and quantification were performed by inductively coupled plasma mass spectrometry (ICP-MS) on a Finnigan Element2 ICP-MS. Protein samples were passed through a Chelex 100 column prior to analysis to remove any unbound metal ions present in the sample. Samples of buffer alone were also analyzed.

Crystallization and Data Collection. Two different crystal forms were obtained using vapor diffusion (*10*). For both crystal forms, the protein drops consisted of 4 μL drops of the reservoir solution mixed with an equal volume of PHS at a 75 mg/mL concentration, as determined using a calculated extinction coefficient of 88 200 M^{-1} cm^{-1} at 280 nm (*10*). Crystals in an *R*32 space group were obtained when the reservoir consisted of 200 mM citric acid at pH 5.0, 260−280 mM ammonium sulfate, and 15%(v/v) glycerol. Optimal conditions for the crystal growth of PHS in a *P*1 form were obtained with a reservoir solution containing 100 mM sodium citrate (pH 5.0), 6.0% (v/v) 2-propanol, 12% (w/v) poly(ethylene glycol) 4000, and 15% (v/v) glycerol (*10*).

Crystals suitable for X-ray analysis grew within 7−10 days and were approximately 0.5 mm in length. The crystals had the characteristic blue color, and the protein was shown to be fully active after the crystals were dissolved. The *R*32 crystals had unit cell constants of a and $b = 294.2$ and $c = 109.5$ Å (*10*). The *P*1 crystals had unit-cell parameters of $a = 109.5$, $b = 163.5$, $c = 164.4$ Å, $\alpha = 117.0$, $\beta = 95.7$, and $\gamma = 107.2°$ ((*10*) and Table 1).

The crystals were looped out of the mother liquor and soaked for 2 min in a cryoprotectant solution consisting of 100 mM sodium citrate (pH 5.0), 8% (v/v) 2-propanol, 12% (w/v) poly(ethylene glycol) 4000, and 30% (v/v) glycerol. The crystals were cryo-cooled in nitrogen gas steam at 110 K. The highest resolution data was collected on a Rigaku R-AXIS IV++ image-plate area detector using Cu Kα radiation from a Rigaku RU-200HB rotating-anode X-ray generator. The X-ray source was equipped with an Osmic confocal mirror assembly. The *R*32 crystals diffracted to a resolution limit of 3.35 Å (*10*), whereas the *P*1 crystals diffracted to a much higher resolution limit of 2.3 Å (Table 1). Although the crystals were frozen, radiation damage limited the completeness of the *P*1 native data to 86.3%. The *R*32 crystals had 2 PHS subunits per asymmetric unit, whereas the *P*1 crystals had 12 PHS subunits per asymmetric unit.

To identify the location of the copper atoms, anomalous data from the *P*1 crystals were collected at the Advanced Light Source (Berkeley, CA) using an ADSC Q210 detector. Complete data sets were collected at three different wave-

Table 1: Final Refinement Statistics Obtained for the PHS Model

data collection	high resolution	peak	edge	remote
Beamline		ALS 8.3.1	ALS 8.3.1	ALS 8.3.1
wavelength (Å)	1.5418	1.37798	1.37923	1.30537
space group	*P*1			
unit-cell parameters (Å, °)	$a = 109.5$, $b = 163.5$, $c = 164.4$, $\alpha = 117.0$, $\beta = 95.7$, $\gamma = 107.2$			
resolution (Å)	2.30	2.80	3.00	2.80
R_{sym}[b] (%)	0.058 (0.284)[a]	0.096 (0.383)	0.098 (0.484)	0.115 (0.707)
number of reflections	339552 (20640)	222734 (30865)	138808 (9936)	162095 (10219)
completeness (%)	86.34 (71.41)	96.0 (91.1)	73.2 (35.8)	70.1 (30.2)
redundancy	2.4 (2.2)	7.3 (5.5)	3.1 (2.5)	3.0 (2.2)
average intensity ($I/\sigma(I)$)	11.3 (2.6)	21.5 (3.8)	11.4 (1.8)	9.9 (1.2)

[a] Values in parentheses are for the last 0.1 Å resolution shell. [b] $R_{sym} = \sum|I-\langle I\rangle|/\sum\langle I\rangle$, where I is the intensity and $\langle I\rangle$ the average intensity for equivalent reflections.

lengths: the f″ peak position at 1.37798 Å, the f′ inflection position at 1.37923 Å, and a high-energy remote position at 1.30537 Å. All diffraction data were integrated with MOSFLM (*14*) and scaled with SCALA (*15*).

Structural Analysis. Initial phases for PHS were obtained using the molecular replacement method with the 3D structure (protein only) of CotA from *B. subtilis* used as the search model (*9*). A clear molecular replacement solution for 2 PHS subunits in the asymmetric unit was obtained using CNS (*16*) for the *R*32 data (*10*). The residues of the CotA molecules were altered to reflect the sequence of PHS, and the type 1 copper center was added. After repeated rounds of refinement using CNS (*16*), a working model of PHS was obtained with an *R*-factor of 34.2% and a free *R*-factor of 38.9%. Using the symmetry of the *R*32 cell, two PHS hexamers were generated from the two PHS subunits in the asymmetric unit using XtalView (*17*). The PHS hexamer, with the copper atoms removed, was used as a search model for a molecular replacement search conducted with the *P*1 data and MOLREP (*18*). The search yielded the solutions for two independent hexamers in the *P*1 unit cell. In the *P*1 cell, additional PHS residues were built using program O. Initial refinement of the model was conducted using CNS (*16*) with strict NCS constraints. Final rounds of refinement were conducted with REFMAC (*19*) using tight NCS restraints for both main and side chain atoms. ARP_waters (*20*) was used to add water molecules to the final model. To rule out model bias, the final model and maps were compared to a model and prime and switch map produced by RESOLVE (*21*). The C and D subunits of the PHS hexamer were used as the primary subunits throughout model building and refinement. All other subunits were added using NCS matrixes derived from CNS (*16*) and the coordinates generated with PDBSET (*22*). During model building, after each refinement using the NCS matrixes, the twelve proteins were subsequently refined with no constraints, and new NCS matrixes were calculated. The final *P*1 model had an *R*-factor of 16.0% and a free *R*-factor of 22.6% (Table 2).

Table 2: Refinement Statistics

resolution (Å)	50−2.3
R_{work} (%)	16.0 (21.8)[a]
R_{free} (%)	22.6 (32.5)
number of nonhydrogen atoms used in refinement	59442
number of protein/heteroatoms/water atoms	54648/144/4650
mean *B* value of model (Å^2)	40.28
rms bond length deviation (Å^2)	0.022
correlation coefficient *Fo*−*Fc*	0.959
correlation coefficient *Fo*−*Fc* Free	0.917

[a] Values in parentheses are for the last 0.1 Å shell.

The *P*1 model, with all copper atoms and water molecules removed, was refined using the anomalous data. One round of rigid-body refinement and two rounds of restrained refinement were performed using REFMAC (*19*). Using the programs CAD and FFT (*22*), the calculated phases of this PHS model were used in combination with the various anomalous difference data (inflection-peak, inflection-remote, and peak-remote) to produce an anomalous electron density map.

Additional Programs. Domain analysis was conducted using the 3D structural neighbor comparison of the VAST algorithm (*23*, *24*). The size and location of the putative substrate-binding pocket was determined using the CASTp server (*25*). Contact regions were analyzed using the program CONTACT contained within the CCP4 package (*22*). Electrostatic calculations were carried out using the program APBS (*26*) with APBS PyMol (*27*). All graphical representations of PHS were prepared using the program PyMol (*27*). The accessible surface area values were computed using the program NACCESS (*28*) with a probe radius of 1.4 Å and a slice width of 0.05 Å. The accessible surface areas were calculated according to the algorithm defined by Lee and Richards (*29*). The changes in the surface areas due to hexamer formation were calculated for two types of surface areas, nonpolar and polar, by comparing the surfaces areas of the hexamer and the monomer from of the protein.

RESULTS

Overall Structure. PHS is a globular protein, with each protein subunit having a size of approximately 75 × 60 × 50 Å^3 (Figure 1). All of the 612 amino acids in the sequence of the mature PHS were modeled except for the first 6 amino acids of the *N*-terminus that starts at residue E31, residues 467−471 that are part of a loop structure, and the *C*-terminal region formed by amino acid residues 629−642, because of a lack of electron density. The structure of PHS can be divided into three domains. Domain 1 is composed of nine beta strands, eight of which form the Greek key β-barrel fold with the additional strand (residues 122−126) forming stabilizing hydrogen bonds with an isolated strand from domain 2 (residues 261−265). The fold of domain 2 (residues 237−412) contains a total of 11 β-strands and closely resembles the classic Greek key β-barrel fold. As with domain 1, an isolated β-strand forms a stabilizing structure with a β-strand from domain 1. Domain 3 (residues 434−628) contains two short helical segments (residues 605−610 and 622−625) as well as 12 strands folded in the common cupredoxin-like topology.

The 3D structure of the subunits of PHS is similar to those of other multicopper oxidases (*30*−*33*) including the *Bacillus subtilis* spore-coat laccase CotA (*9*) used for molecular

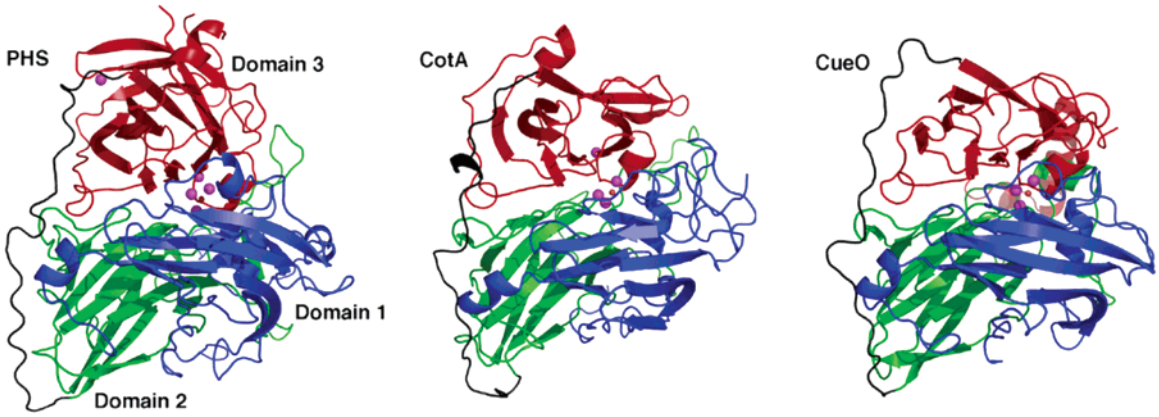

FIGURE 1: Backbone structures of PHS, CotA, and CueO showing the relative arrangement of domain 1 (residues 37−236, blue), domain 2 (residues 237−411, green), domain 3 (residues 439−628, red), the loop connecting domains 2 and 3 (residues 412−438, black), the copper atoms (purple spheres), and the bridging oxygen atom and coordinating water molecule (red spheres) (residue numbers are for PHS sequence). The coordinates of CotA and CueO are from the pdb files 1GSK (*9*) and 1N68 (*3*).

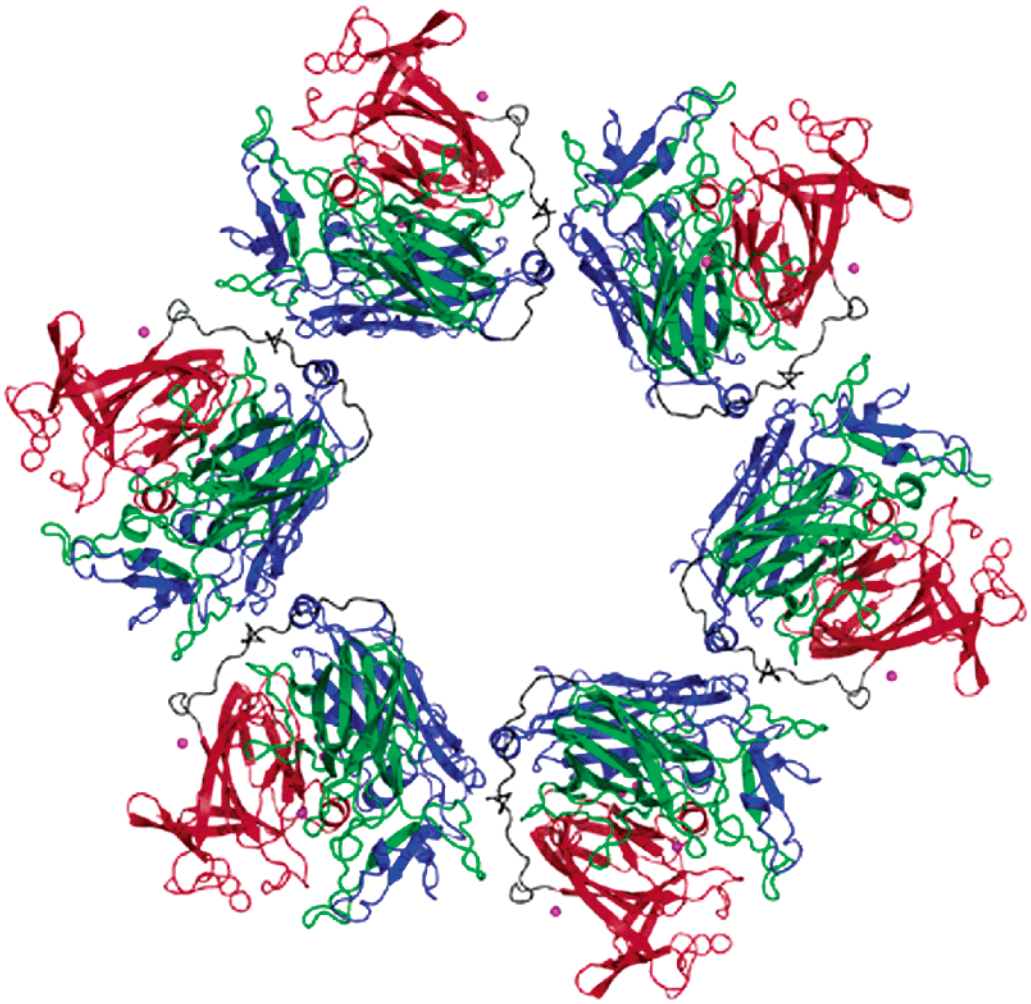

FIGURE 2: Hexameric structure of PHS. The cross-sectional diameter is 185 Å with a 50 Å inner cavity that is unoccupied. The exterior of the hexamer is formed by domain 3 (red), with domain 1 (blue) largely forming the interior as well as the protein−protein contact region with domain 2 (green). The copper cofactors (purple) as well as the coordinating ion or molecule X and water molecule (red) are shown as spheres. Note that the loop extending from domain 1 to 2 (black) contributes to the binding site between the subunits.

replacement, which consists of three cupredoxin-like domains (Figure 1). The cupredoxin-like fold, typified by the blue copper proteins plastocyanin and azurin, is common to the multicopper oxidase family and is mainly composed of an eight-stranded Greek key β-barrel with two β-sheets arranged in a sandwich conformation (*34*). The outstanding feature of the cupredoxin Greek key β-barrel topology compared to that of other Greek key β-barrels is the existence of parallel β-strands (*35*). PHS, with 612 amino acid residues, is significantly larger than other prokaryotic multicopper oxidases such as CueO and CotA that contain 488 and 513 amino acid residues, respectively. The additional residues of PHS do not significantly change the core structure of any of the three domains but rather are within surface loops. One

of these loops connects domains 2 and 3 and spans almost the entire length of the protein (Figure 1). This feature is shared with other prokaryotic multicopper oxidases and, so far, has not been observed in the eukaryotic enzymes laccase, ascorbate oxidase, and ceruloplasmin (*9*). In multicopper oxidases, domain 2 does not contribute any residues to the copper centers, and its primary structural role is to connect the other two domains.

Hexameric Structure. The final refined model consisted of two hexamers with each hexamer spaning a distance of 185 Å across the cross-sectional diameter and a large central cavity with a diameter of 50 Å (Figure 2). Each PHS subunit is arranged with domain 3 on the exterior of the surface and domain 1 largely forming the interior. The six subunits of the hexamer are not crystallographically related but follow an approximate 6-fold rotation about the center. The rotational symmetry is very close, allowing the structure to be initially built as an exact hexamer. After relaxing this constraint, the symmetry was approximately maintained with NCS noncrystallographic symmetry restraints. Rotation and translation of the A subunit using noncrystallographic symmetry operators leads to superposition onto the 11 other subunits with a relatively small rms deviation ranging from 0.304 to 0.412 Å for the F and D subunits, respectively. The largest differences occurred for residues 557−567, which formed loops that are uniquely placed in each subunit and required individual building in electron density.

Domains 1 and 2 are the only domains that participate in the monomer−monomer contacts. Domain 3 forms a protrusion on the outside of the hexameric structure and is not in contact with either of the neighboring monomers. The loop structure that connects domain 1 to domain 2 also contributes to the contact site, particularly the short α-helical segment formed by amino acid residues 226−231. Two small *β*-strands from domains 1 and 2 formed by amino acid residues 122−126 and 261−265, respectively, also contribute to interactions. The residues comprising the contact regions of the individual subunits forming the hexamer are largely charged residues with a small number of hydrophobic residues occupying pockets on the surface of the neighboring subunits. Arginine, aspartic acid, and glutamic acid residues are particularly prominent within the intersubunit contact regions (Figure 3). All of the other bacterial multicopper oxidases are monomers, and among the multicopper oxidases from eukaryotic species, only ascorbate oxidase is dimeric rather than monomeric. The interactions that stabilize the dimer in ascorbate oxidase primarily involve residues that are part of a surface loop that is formed by amino acid residues Ile 182−Lys 194. This loop is not present in PHS or in any of the bacterial enzymes, and the flanking regions in PHS form part of a beta strand in domain 1 that is buried by the amino terminus region. Experiments are underway to determine the structure of PHS in the dimeric form to delineate the factors that control its formation.

Copper Centers. An analysis of the ICP-MS data showed the presence of five copper atoms per protein subunit with the content of all other metals being negligible. The electron density map clearly shows that PHS contains a total of five metal atoms (Figure 4). Four of these metal atoms are located primarily in domains 1 and 3 and correspond to the copper centers that have been observed in other multicopper oxidases. These copper atoms form one mononuclear type 1 center, one mononuclear type 2 center, and one binuclear type 3 copper center. The fifth metal atom is found in the loop connecting domains 2 and 3 and represents a new cofactor not previously described in any other multicopper oxidase. The anomalous diffraction data showed a very strong peak centered at this position allowing the metal to be unambiguously assigned as copper. These data also verified the assignment of the other four metals as copper. Thus, both the ICP-MS and the anomalous X-ray data show that PHS has a total of five copper atoms with well-defined coordinations. On the basis of the coordination of the fifth copper, it was expected to be a type 2 center.

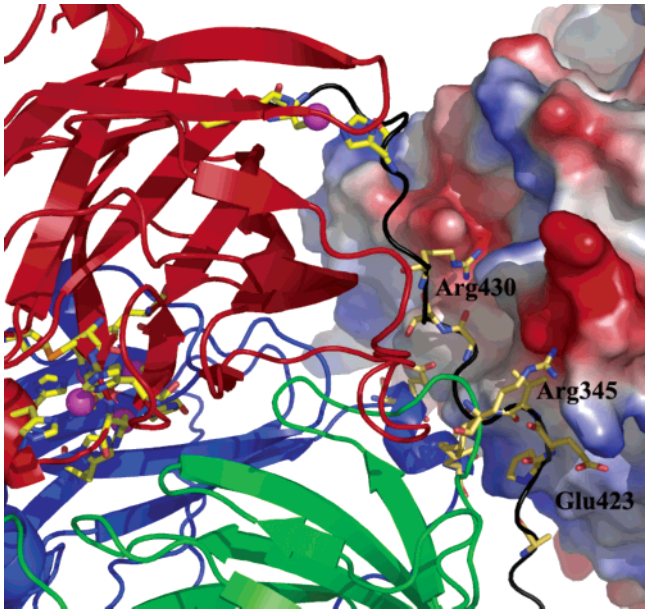

FIGURE 3: Contact region between neighboring subunits of the hexamers. The backbone of one subunit (A) is shown (colored by domains, as in Figure 1) with the new type 2 copper atom (purple sphere) and three coordinating histidines (colored by atom type).

The type 1 copper center, identified as Cu1, has four ligands (His524, His608, Cys603, and Met613) that are entirely from domain 3 (Figure 5). The geometry of the type 1 center is a distorted bypyramidal with a missing axial ligand common to type 1 copper centers. Among these residues, only the axial methionine ligand is not conserved among the multicopper oxidases. Although this ligand is methionine in most multicopper oxidases, in some laccases, this residue can also be leucine or phenylalanine (*36*). The bond distances in PHS (Figure 5) are similar to those found in other multicopper oxidases (*9*). As a part of domain 3, the type 1 center is contained in the protrusion on the outside of the hexameric structure and is located directly below the putative binding pocket (see below). The type 1 copper center is 12.5 Å away from Cu2 of the type 3 center and is connected to the type 3 center through the HCH motif that facilitates the transfer of electrons from the type 1 to the type 3 center (*2*).

Despite the presence of conserved histidine residues in the primary sequence, PHS was thought to not contain a type 3 center on the basis of spectroscopic studies. The electron density provides clear evidence for two copper atoms with a bridging ligand, which has not been unambiguously identified but has initially been modeled as OH, although other ligands such as water or various anions would be

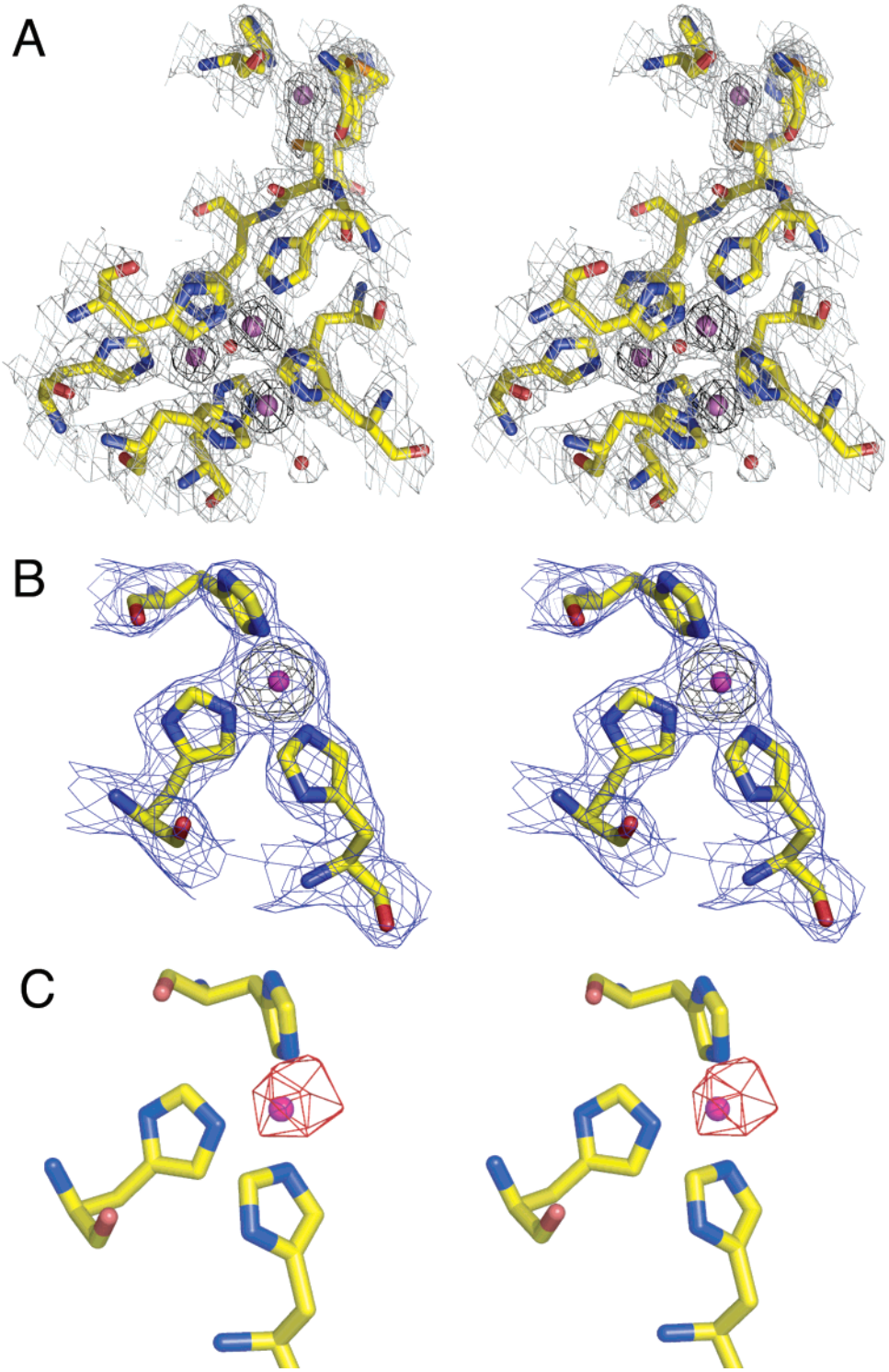

FIGURE 4: Stereoviews of the electron density and the model for the four conserved copper centers (A) and the new type 2 center (B) with the coordinating ligands. These electron density maps are shown at both the 1.5 σ (blue) and 4.5 σ (black) contour level. (C) Anomalous electron density map for copper showing a large 16 σ (red) peak at the same position as the new copper center. The three histidines, 434, 438, and 440, and the metal are shown in the same view as that in (B) and (C).

compatible with the electron density (Figure 4a). The 3.88 Å distance between the two copper atoms, which are identified as Cu2 and Cu3, and the Cu2-X-Cu3 bond angle of 153.14° are comparable to those found in other multicopper oxidases (Figure 5). The six histidine ligands have distances similar to those in the other multicopper oxidases. Located near the type 3 center is a type 2 center (Figure 4). The copper atom of the type 2 center, identified as Cu4, is 3.63 and 3.86 Å away from the Cu2 and Cu3 copper atoms, respectively. Domains 1 and 3 provide the two coordinating histidines, His161 and His527, and a water molecule provides a third ligand. The trinuclear cluster of PHS has coordination geometries and copper−copper distances similar to those of other multicopper oxidases.

The fifth copper atom is a part of a type 2 center and coordinated by three histidines with a T-shape coordination (Figure 4). Two of the three coordinating histidines, His434 and His438, are a part of the loop structure that connects

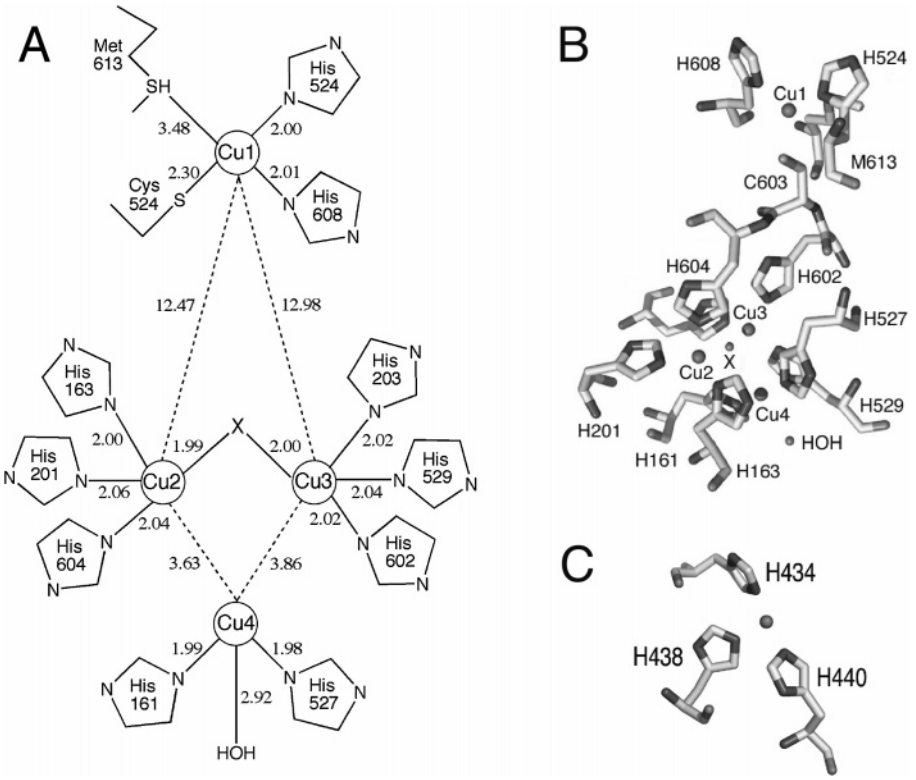

FIGURE 5: Copper centers including the coordinating ligands. (A) Diagram of the arrangement of the four conserved copper atoms, the distances to the ligating atoms, and the distances between the copper atoms. (B) Four conserved copper atoms and their surrounding ligands (shaded by atom type). The view is the same as that in Figure 4A. (C) New type 2 copper atom and the three histidine ligands (shaded by atom type). X represents an unidentified bridging ligand such as OH. Views are the same as Figure 4.

domains 2 and 3, a part of which interacts with the neighboring subunit of the hexamer. The third histidine, His440, is located at the start of the first β-strand of domain 3. When the copper atom is bound, the His ligands act to form a kink at the end of the connecting loop and anchor the end of the loop directly to domain 3. This loop/kink structure is further stabilized by a hydrogen bond between the carbonyl oxygen of the Ile436 and the Nδ atom of His438.

EPR spectra of PHS showed a complex signal centered around $g = 2$, characteristic of both type 1 and type 2 copper centers (data not shown). A total of 5 spins (1 spin/Cu) were determined from the EPR experiments.

Substrate Binding Pocket and Solvent Channels. Possible substrate binding pockets were identified using the CASTp server (*25*). One putative substrate binding pocket was found on the surface of domain 3 and near the type 1 copper center. This pocket is primarily formed by amino acid residues from three segments: Ser 278 to Pro 281, Pro 448 to Pro 457, and Glu 601 to Met 611. The amino acid residue Met611 extends over the top of the binding pocket, forming a bridge-like structure that creates three openings into the binding pocket. The binding pocket is partially obstructed by a surface loop formed by amino acid residues 265−281. The location of this binding pocket agrees with the adduct binding site found in the crystal structure of CotA with bound 2,2′-azinobis-(3-ethylbenzothiazoline-6-sulfonate (*37*). The binding pocket of PHS has a solvent accessible area of 294 Å^2 and a molecular surface area of 493 Å^2; therefore, it is not as large as that of CotA (468 and 743 Å^2, respectively (*9*)) and is closer in size to that of the *C. cinereus* laccase (206 and 383 Å^2, respectively (*9*)). The long and narrow shape of the binding pocket probably reflects the restrictive substrate specificity of PHS relative to CotA.

PHS and other multicopper oxidases have well-defined solvent channels that allow for the transport of O_2 between the protein surface and the buried trinuclear copper center. In PHS, two channels connect the Cu3 and Cu4 of the trinuclear center to the surface of the protein. Both channels lead to surface openings located in depressions with a number of bound water molecules and are formed by the interface of domains. The channel connecting Cu3 to the surface runs through the interface of domains 1 and 3 and leads to a surface cavity located on domain 1. The channel connecting Cu4 to the surface runs through the interface of domains 2 and 3 and leads to a cavity on the surface of domain 3.

DISCUSSION

The structure of PHS has been solved at a resolution limit of 2.3 Å. Despite the relatively low sequence homology of PHS to other multicopper oxidases, the overall fold of PHS is similar to those of other members of this family. The structure reveals two features that are critical to understanding the enzymatic activity. First, the structure shows the presence of five copper atoms, including the presence of a type 3 center that had been previously thought unlikely on the basis of spectroscopic data. Second, PHS contains a novel type 2 center that appears to play a critical role in the stabilization of the hexameric form of the protein that is much more active than the dimeric form. These two points are discussed below.

PHS has been considered a member of the multicopper oxidase family on the basis of spectroscopic analysis, catalytic mechanisms, and conserved domains within the

primary sequence (*2*, *7*, *8*, *38*). All multicopper oxidases with known structures contain a type 1 center and a type 2/type 3 trinuclear cluster. However, because of the lack of a 330 nm absorption band, the presence of a binuclear type 3 center in PHS remained unclear even though the alignment of the sequence of PHS with those of the other multicopper oxidases indicated that all of the conserved ligands for the type 1, type 2, and binuclear type 3 copper centers were present in the primary sequence of PHS (*2*). All three types of copper centers were found in the crystal structure of PHS with distances and geometries similar to those of other multicopper oxidases, providing for the first time direct evidence of a type 3 copper center in this enzyme.

ICP-MS and EPR studies conducted at pH 6 indicate the presence of five Cu atoms per subunit and approximately 1 spin/Cu as types 1 and 2 but not type 3, as previously observed by Freeman et al. (*8*). In contrast, other multicopper oxidases have a type 3 center with an absorption band at 330 nm that is a hydroxide bridged, antiferromagnetically coupled binuclear copper(II) center, and therefore, they are EPR inactive. The spectroscopic properties of Cu centers in proteins is strongly dependent on the coordination of the metal ions (*39*). The lack of a 330 nm absorption band in PHS implies a lack of a hydroxide bridge between the two copper ions in the putative type 3 center, suggesting that the observed density between Cu2 and Cu3 is not a hydroxide ion but another small ion or molecule. The EPR spectrum of PHS shows that all Cu ions are paramagnetic, indicating that the two Cu ions in the type 3 center are either uncoupled or weakly coupled and, therefore, are paramagnetic. Experiments to identify the bridging ligand between Cu2 and Cu3 in PHS are currently underway.

The structure of PHS reveals the presence of a fifth copper atom. This copper atom is coordinated by three histidines, H434, H438, and H440, in a T-shape geometry. This geometry is commonly found for Cu(I) coordination compounds but unusual for copper-containing proteins (*40*). There is space available in the structure for a water molecule to serve as a fourth ligand, which will make the coordination square planar. The resolution is not sufficient to unambiguously position the water molecule, and therefore, it was not included in the structure. On the basis of the EPR data, we would expect this copper to be Cu(II). Hence, either the copper has a fourth water ligand or the copper has been reduced to Cu(I) by X-ray radiation. To resolve this ambiguity, we plan to perform EPR studies on the crystals before and after exposure to X-rays. Also planned is the determination of the oxidation/reduction potentials of the five copper atoms.

The presence of additional copper centers have been documented in two of the other multicopper oxidases with known structures, ceruloplasmin and CueO (*41*, *42*). Ceruloplasmin contains two additional type 1 centers in domains 2 and 4, although the distance to the trinuclear center from these type 1 centers is larger than that of the type 1 center in domain 6. Furthermore, two additional metal binding sites, termed labile cation sites, have been described. These two sites appear only partially occupied in the crystal structure, and it has been speculated that these sites may be utilized for copper transport in a manner independent of protein turnover (*41*). In CueO, an additional copper site is found in a methionine-rich region. This Cu atom is coordinated in a trigonal bipyramidal fashion by two methionines, two aspartates, and a water molecule. This site is only 7.5 Å away from the type 1 copper site, and mutations to the coordinating residues of this labile copper result in the loss of oxidation and copper tolerance, confirming a regulatory role for this site (*42*).

PHS is unique among the multicopper oxidases in that it exists in two oligomeric forms with distinct catalytic activities: low activity dimers and high activity hexamers. A comparison to other hexameric proteins provides insight into the factors that stabilize the hexameric form. Studies conducted with the hexameric inorganic pyrophosphatase from *S. acidocaldarius* and *E. coli* showed that increased hydrogen bonding and buried surface area accounted for the increased stability of the hexamers (*43*, *44*). The number of contacts in the PHS hexamer is clearly greater than what would be expected in the dimer. The presence of the large cavity is unexpected on the basis of the function of this enzyme and the normal tight packing usually observed in multimeric proteins.

The hexameric form is the most active form of PHS and requires 4−5 Cu atoms per subunit for maximum activity (*1*, *8*). The fifth copper atom, Cu5, is incorporated into a new type 2 copper center that is located at the end of the loop connecting domains 2 and 3. This center is approximately 25 Å from both Cu1 and Cu4 (Figure 1) and is unlikely to play a role in the transfer of electrons to the substrate. Instead, this copper center appears to play a role in stabilizing the hexamer through its interactions with the loop connecting domains 1 and 2. The binding of the copper atom constrains the loop connecting domains 2 and 3 by creating a kink in the loop (Figure 5). This kink is further stabilized by a hydrogen bond between the carbonyl oxygen of the Ile436 and the Nδ atom of His438. These interactions would help stabilize the hexamer by firmly anchoring the loop to domain 3. Studies conducted with human immunoglobulin show that hydrogen bonds in surface loops can stabilize entire domains by constraining the movement of the loop structure (*45*). The same study showed that hydrogen bonds between main-chain and side-chain atoms increased the stability of the protein. In the case of PHS, the mechanism of constraining the loop is different (metal binding vs. hydrogen bonding), but both situations result in a constrained surface loop.

The high activity of the hexameric form is likely due to a number of factors, including the stabilization of this form of the protein relative to the dimer. Accessibility of the active site, geometry of the copper centers, and the availability of proper solvent channels may also play an important role in the regulation of PHS. The structure of the hexameric form of PHS provides a new template for understanding the mechanism of multicopper oxidases and the stabilization of higher order oligomeric proteins by metals. The results of these studies are expected to lead to a better understanding of multielectron transfer in biological systems, including the catalytic reduction of oxygen to water and their regulation by cellular processes.

ACKNOWLEDGMENTS

We wish to thank Charles Olea Jr. for assistance at the beginning of this project and Dario Cabrera and Kevin J.

Smith for the purification of PHS. We thank Russell LoBrutto for EPR data collection and analysis. We thank George H. Jones (Emory University) for providing the overproducing strain of *S. lividans*. We are grateful to the Advanced Light Source (ALS) for their support of our access to Beamline 8.3.1 of ALS at Lawrence Berkeley National Laboratory (Berkeley, CA). The ALS is operated by the Department of Energy and supported by the National Institute of Health.

REFERENCES

1. Choy, H. A., and Jones, G. H. (1981) Phenoxazinone synthase from *Streptomyces antibioticus*: purification of the large and small enzyme forms, *Arch. Biochem. Biophys. 211*, 55−65.
2. Solomon, E. I., Sundaram, U. M., and Machonkin, T. E. (1996) Multicopper oxidases and oxygenases, *Chem. Rev. 96*, 2563−2605.
3. Roberts, S. A., Weichsel, A., Grass, G., Thakali, K., Hazzard, J. T., Tollin, G., Rensing, C., and Montfort, W. R. (2002) Crystal structure and electron-transfer kinetics of CueO, a multicopper oxidase required for copper homeostasis in *Escherichia coli*, *Proc. Natl. Acad. Sci. U.S.A. 99*, 2766−2771.
4. Enguita, F. J., Matias, P. M., Martins, L. O., Placido, D., Henriques, A. O., and Carrondo, M. A. (2002) Sporecoat laccase CotA from *Bacillus subtilis*: crystallization and preliminary X-ray characterization by the MAD method, *Acta Crystallogr., Sect. D 58*, 1490−1493.
5. Messerschmidt, A., Rossi, A., Ladenstein, R., Huber, R., Bolognesi, M., Gatti, G., Marchesini, A., Petruzzelli, R., and Finazziagro, A. (1989) X-ray crystal-structure of the blue oxidase ascorbate oxidase from zucchini−Analysis of the polypeptide fold and a model of the copper sites and ligands, *J. Mol. Bio. 206*, 513−529.
6. Spira-Solomon, D. J., Allendorf, M. D., and Solomon, E. I. (1986) Low-temperature magnetic circular dichroism studies of native laccase: Confirmation of a trinuclear copper active site, *J. Am. Chem. Soc. 108*, 5318−5328.
7. Barry, C. E., Nayar, P. G., and Begley, T. P. (1989) Phenoxazinone synthase: mechanism for the formation of the phenoxazinone chromophore of actinomycin, *Biochemistry 28*, 6323−6333.
8. Freeman, J. C., Nayar, P. G., Begley, T. P., and Villafranca, J. J. (1993) Stoichiometry and spectroscopic identity of copper centers in phenoxazinone synthase: A new addition to the blue copper oxidase family, *Biochemistry 32*, 4826−4830.
9. Enguita, F. J., Martins, L. O., Henriques, A. O., and Carrondo, M. A. (2003) Crystal structure of a bacterial endospore coat component: a laccase with enhanced thermostability properties, *J. Biol. Chem. 278*, 19416−19425.
10. Smith, A. W., Camara-Artigas, A., Olea, C., Francisco, W. A., and Allen, J. P. (2004) Crystallization and initial X-ray analysis of phenoxazinone synthase from *Streptomyces antibioticus*, *Acta Crystallogr., Sect. D 60*, 1453−1455.
11. Jones, G. H., and Hopwood, D. A. (1984) Molecular cloning and expression of the phenoxazinone synthase gene from *Streptomyces antibioticus*, *J. Biol. Chem. 259*, 4151−4157.
12. Gallo, M., and Katz, E. (1972) Regulation of secondary metabolite biosynthesis: catabolite repression of phenoxazinone synthase and actinomycin formation by glucose, *J. Bacteriol. 109*, 659−667.
13. Katz, E., and Goss, W. A. (1959) Controlled biosynthesis of actinomycin with sarcosine, *Biochem. J. 73*, 458−465.
14. Leslie, A. G. W. (1992) Recent changes to the MOSFLM package for processing film and image plate data, *Jnt. CCP4/ESF-EACBM Newslett. Protein Crystallogr. 26*, 27−33.
15. Evans, P. R. (1997) SCALA, *Jnt. CCP4/ ESF-EACBM Newslett. Protein Crystallogr. 33*, 22−24.
16. Brünger, A. T., Adams, P. D., Clore, G. M., DeLano, W. L., Gros, P., Grosse-Kunstleve, R. W., Jiang, J. S., Kuszewski, J., Nilges, M., Pannu, N. S., Read, R. J., Rice, L. M., Simonson, T., and Warren, G. L. (1998) Crystallography & NMR system: A new software suite for macromolecular structure determination, *Acta Crystallogr., Sect. D 54*, 905−921.
17. McRee, D. E. (1999) XtalView Xfit − a versatile program for manipulating atomic coordinates and electron density, *J. Struct. Biol. 125*, 156−165.
18. Vagin, A., and Teplyakov, A. (1997) MOLREP: an automated program for molecular replacement, *J. Appl. Crystallogr. 30*, 1022−1025.
19. Winn, M. D., Murshudov, G. N., and Papiz, M. Z. (2003) Macromolecular TLS refinement in REFMAC at moderate resolutions, *Methods Enzymol. 374*, 300−321.
20. Morris, R. J., Perrakis, A., and Lamzin, V. S. (2003) ARP/wARP and automatic interpretation of protein electron density maps, *Methods Enzymol. 374*, 229−244.
21. Terwilliger, T. C. (2003) SOLVE and RESOLVE: Automated structure solution and density modification, *Methods Enzymol. 374*, 22−37.
22. Collaborative computational project, Number 4 (1994) The CCP4 suite − programs for protein crystallography, *Acta Crystallogr., Sect. D 50*, 760−763.
23. Gibrat, J. F., Madej, T., and Bryant, S. H. (1996) Surprising similarities in structure comparison, *Curr. Opin. Struct. Biol. 6*, 377−385.
24. Gibrat, J. F., Madej, T., Spouge, J. L., and Bryant, S. H. (1997) The vast protein structure comparison method, *Biophys. J. 72*, M-Pos298.
25. Liang, J., Edelsbrunner, H., and Woodward, C. (1998) Anatomy of protein pockets and cavities: measurement of binding site geometry and implications for ligand design, *Protein Sci. 7*, 1884−1897.
26. Baker, N. A., Sept, D., Joseph, S., Holst, M. J., and McCammon, J. A. (2001) Electrostatics of nanosystems: application to microtubules and the ribosome, *Proc. Natl. Acad. Sci. U.S.A. 98*, 10037−10041.
27. DeLano, W. L. (2002), The PyMol molecular graphics system, DeLano Scientific, San Carlos, CA.
28. Hubbard, S. J., and Thornton, J. M. (1993), NACCESS, Department of Biochemistry and Molecular Biology, University College, London.
29. Lee, B., and Richards, F. M. (1971) Interpretation of protein structures − Estimation of static accessibility, *J. Mol. Biol. 55*, 379−380.
30. Hakulinen, N., Kiiskinen, L. L., Kruus, K., Saloheimo, M., Paananen, A., Koivula, A., and Rouvinen, J. (2002) Crystal structure of a laccase from *Melanocarpus albomyces* with an intact trinuclear copper site, *Nat. Struct. Biol. 9*, 601−605.
31. Messerschmidt, A., Ladenstein, R., Huber, R., Bolognesi, M., Avigliano, L., Petruzzelli, R., Rossi, A., and Finazziagro, A. (1992) Refined crystal structure of ascorbate axidase at 1.9 Å resolution, *J. Mol. Biol. 224*, 179−205.
32. Piontek, K., Antorini, M., and Choinowski, T. (2002) Crystal structure of a laccase from the fungus *Trametes versicolor* at 1.90-angstrom resolution containing a full complement of coppers, *J. Biol. Chem. 277*, 37663−37669.
33. Zaitseva, I., Zaitsev, V., Card, G., Moshkov, K., Bax, B., Ralph, A., and Lindley, P. (1996) The X-ray structure of human serum ceruloplasmin at 3.1 Å: Nature of the copper centres, *J. Inorg. Biol. Chem. 1*, 15−23.
34. Lindley, P. F. (2001) Multicopper oxidases, in *Handbook on metalloproteins* (Bertini, I., Sigel, A., and Sigel, H., Eds.) pp 763−8111, Marcel Dekker, Inc., New York.
35. Murphy, M. E. P., Lindley, P. F., and Adman, E. T. (1997) Structural comparison of cupredoxin domains: domain recycling to construct proteins with novel functions, *Protein Sci. 6*, 761−770.
36. Xu, F., Berka, R. M., Wahleithner, J. A., Nelson, B. A., Shuster, J. R., Brown, S. H., Palmer, A. E., and Solomon, E. I. (1998) Site-directed mutations in fungal laccase: effect on redox potential, activity and pH profile, *Biochem. J. 334*, 63−70.
37. Enguita, F. J., Marcal, D., Martins, L. O., Grenha, R., Henriques, A. O., Lindley, P. F., and Carrondo, M. A. (2004) Substrate and dioxygen binding to the endospore coat laccase from *Bacillus subtilis*, *J. Biol. Chem. 279*, 23472−23476.
38. Villafranca, J. J., Freeman, J. C., and Kotchevar, A. (1993) Copper-containing enzymes: structure and mechanism, in *Bioinorganic Chemistry of Copper* (Karlin, D. K., and Tyeklar, Z., Eds.) pp 439−446, Chapman and Hall, New York.
39. Solomon, E. I., Baldwin, M. J., and Lowery, M. D. (1992) Electronic structures of active sites in copper proteins: contributions to reactivity, *Chem. Rev. 92*, 521−542.
40. Rulisek, L., and Vondrasek, J. (1998) Coordination geometries of selected transition metal ions (Co^{2+}, Ni^{2+}, Cu^{2+}, Zn^{2+}, Cd^{2+}, and Hg^{2+}) in metalloproteins, *J. Inorg. Biochem. 71*, 115−127.
41. Lindley, P. F., Card, G., Zaitseva, I., Zaitsev, V., Reinhammar, B., SelinLindgren, E., and Yoshida, K. (1997) An X-ray structural

study of human ceruloplasmin in relation to ferroxidase activity, *J. Biol. Inorg. Chem. 2*, 454−463.
42. Roberts, S. A., Wildner, G. F., Grass, G., Weichsel, A., Ambrus, A., Rensing, C., and Montfort, W. R. (2003) A labile regulatory copper ion lies near the T1 copper site in the multicopper oxidase CueO, *J. Biol. Chem. 278*, 31958−31963.
43. Leppanen, V. M., Nummelin, H., Hansen, T., Lahti, R., Schafer, G., and Goldman, A. (1999) *Sulfolobus* acidocaldarius inorganic pyrophosphatase: structure, thermostability, and effect of metal ion in an archael pyrophosphatase, *Protein Sci. 8*, 1218−1231.
44. Kankare, J., Salminen, T., Lahti, R., Cooperman, B. S., Baykov, A. A., and Goldman, A. (1996) Structure of *Escherichia coli* inorganic pyrophosphatase at 2.2 Å resolution, *Acta Crystallogr., Sect. D 52*, 551−563.
45. Pokkuluri, P. R., Raffen, R., Dieckman, L., Boogaard, C., Stevens, F. J., and Schiffer, M. (2002) Increasing protein stability by polar surface residues: domain-wide consequences of interactions within a loop, *Biophys. J. 82*, 391−398.

BI0525526